XIV-th International School-Conference
“Actual Problems of Microworld Physics”
12-24 August, Belarus, Grodno region

Measurements of the inclusive jet production cross-section in association with a Z-boson in pp collisions at 8 TeV using the ATLAS detector

Aliaksei Hrynevich

22/08/2018

Outline

1. **Motivation for the Z+jets cross-section measurements**
2. **ATLAS detector**
3. **Electron and jets definitions**
4. **Z+jets theoretical predictions**
5. **Z+jets cross-section measurements**
6. **Summary**

Motivation

$Z \rightarrow ee$ + inclusive jets ($N_{jets} \geq 1$) double differential cross-section is measured as a function of absolute jet rapidity ($|y_{jet}|$) in bins of p_T^{jet} using 20.1 fb^{-1} 8 TeV ATLAS pp collisions data.

Process diagrams

qqbar -> Z+jet

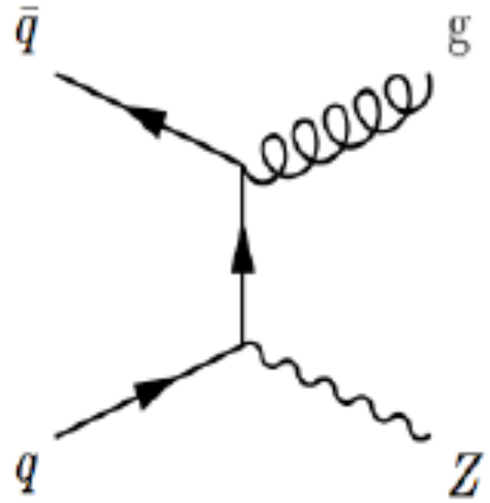

qg -> Z+jet

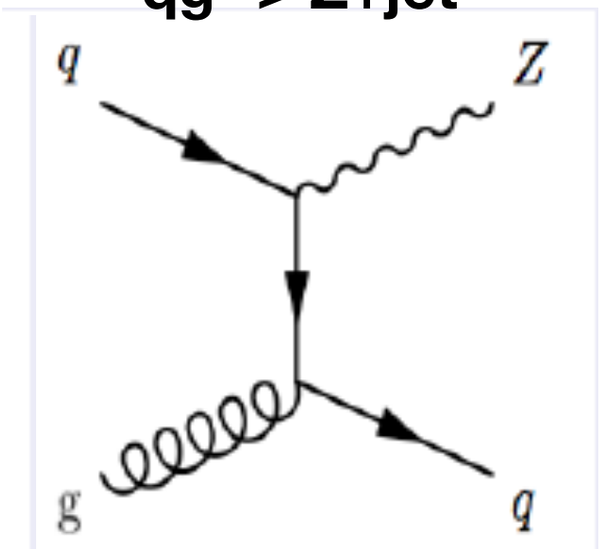

The measurement

- is sensitive to the gluon density and provides an input for gluon PDF constraints
- explores a new phase-space in Z+jets kinematics
- provides a benchmark for fixed-order calculations and to MC simulations as Z+jets is a large background to various measurements of SM processes

50-90% contribution from quark-gluon initial state

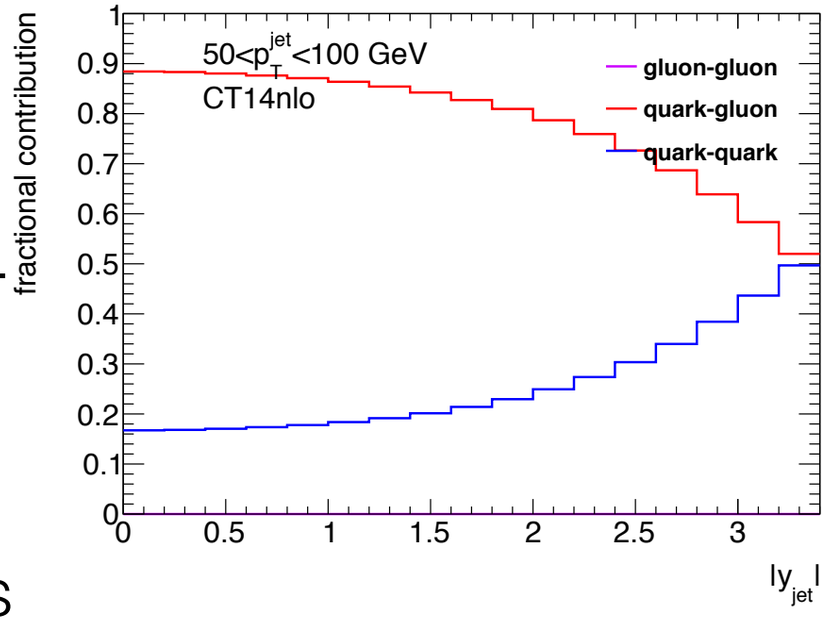

Strongly correlated with gluon PDF

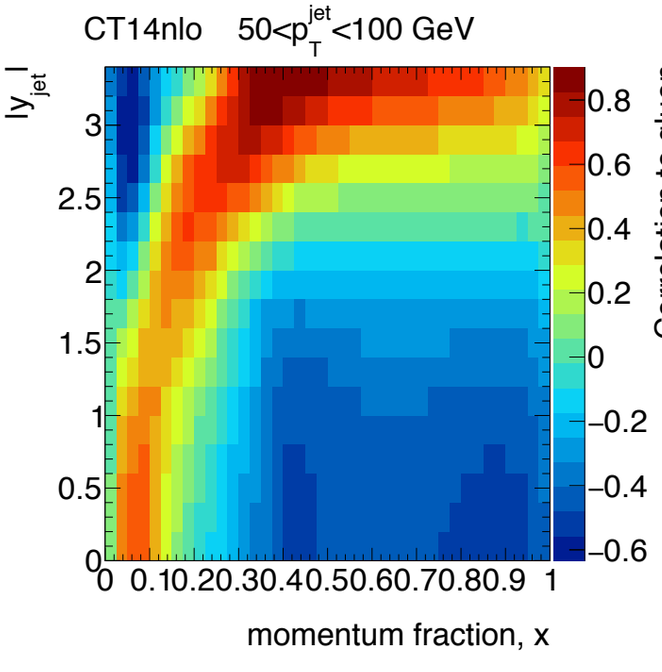

ATLAS detector

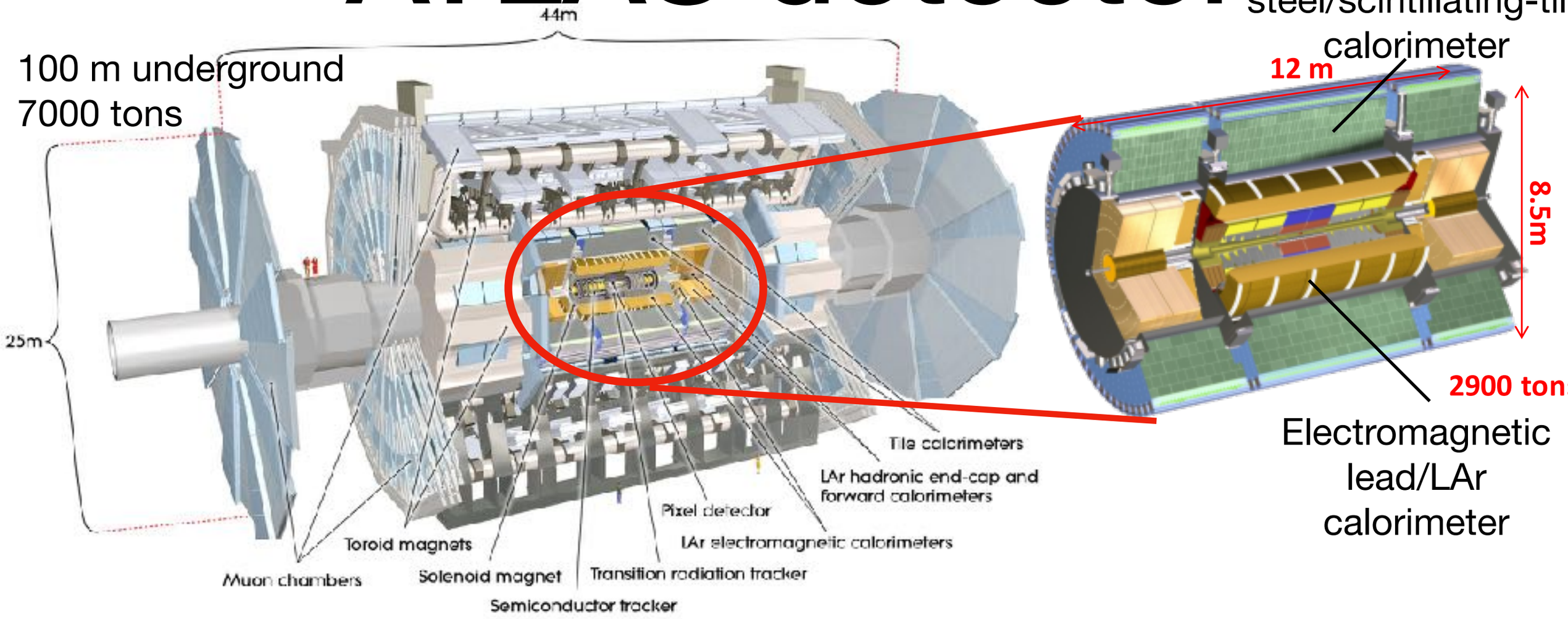

- ATLAS is the multipurpose detector at the LHC
- detection is done by
  - internal tracker (pixel, silicon microstrip tracker, transition radiation tracker). Provides a coverage of $|\eta|<2.5$.

$$\eta = -\ln\tan(\theta/2)$$

  - calorimeters cover $|\eta|<4.9$
    - electromagnetic calorimeter (lead/liquid-argon) up to $|\eta|<3.2$
    - hadronic calorimeter (steel/scintillating-tiles up to $|\eta|<1.7$ + two copper/LAr endcaps)
  - external muon spectrometer covering $|\eta|<2.7$
- Allows for a wide range of high energy physics studies both within the Standard Model and beyond

Electron reconstruction

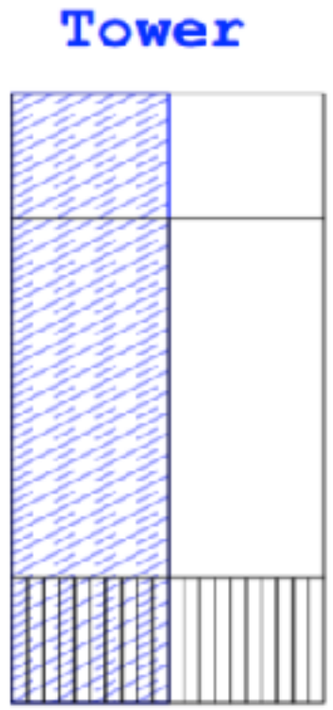

- The electron reconstruction starts from the energy deposits (clusters) in EM calorimeter.
  - The cluster formation starts from towers of size $\Delta\eta$x$\Delta\phi$=0.025x0.025. The energy of all shower-depth layers is summed to provide the energy of a tower.
  - The sliding-window algorithm searches for clusters by a window of 3x5 towers in η-ϕ space seeded by towers with E_T>2.5 GeV (efficiency is >99% for E_T>15 GeV).
- Clusters matched to reconstructed tracks originating from reconstructed vertex are classified as electrons.
- The electron cluster is then rebuilt to 3x7 (barrel) and 5x5 (endcap) towers.

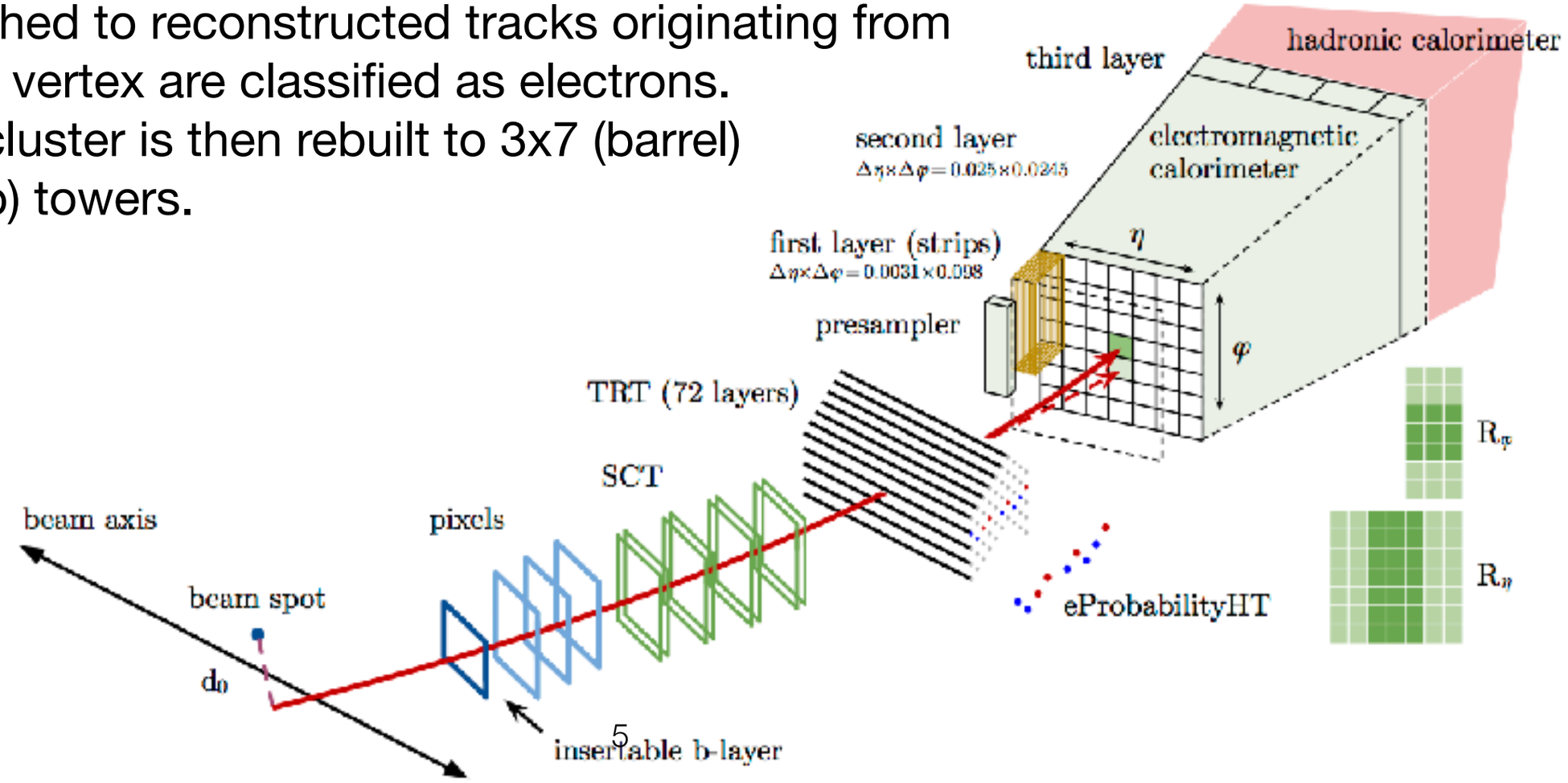

Electron energy measurements and identification

- The electron energy is determined from the energy of the cluster (from cells in different layers) while the η and ϕ coordinates are taken from track.
- The calibration restores the true e energy from the quantities measured by the detector.

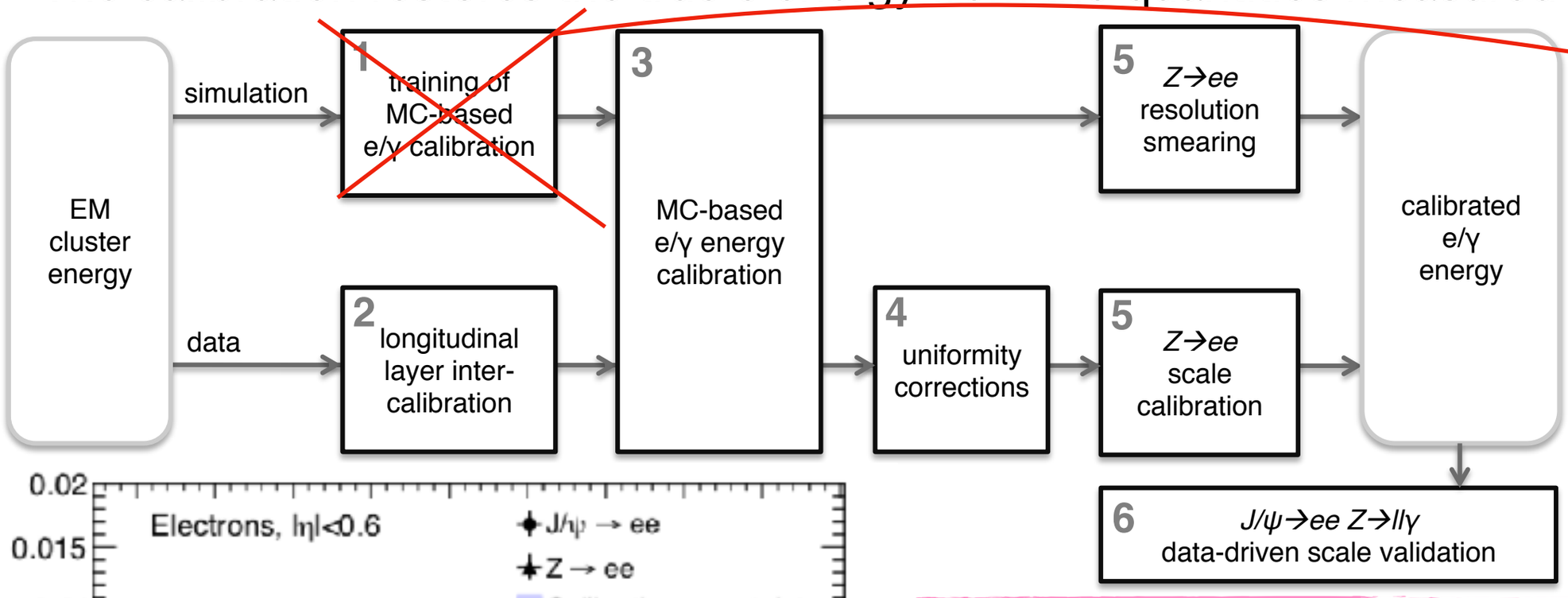

In MC-based calibration a special simulated sample is used where the energy losses in inactive material are preserved.

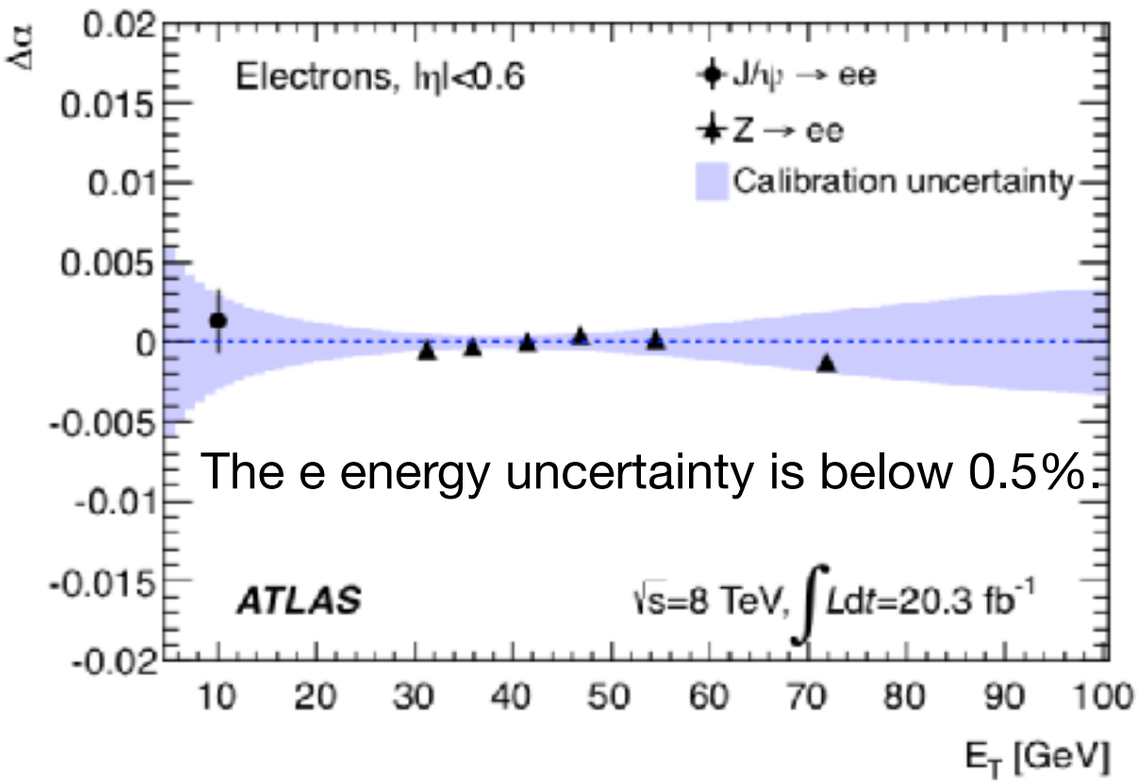

The e energy uncertainty is below 0.5%.

Electron Identification

- Electron identification criteria (loose, medium and tight) are intended to reject photon conversions, heavy hadrons decays and hadrons misidentified as electrons based on the shower shape properties, number of hits in tracker and track-to-cluster matching quality.

Introduction to jets

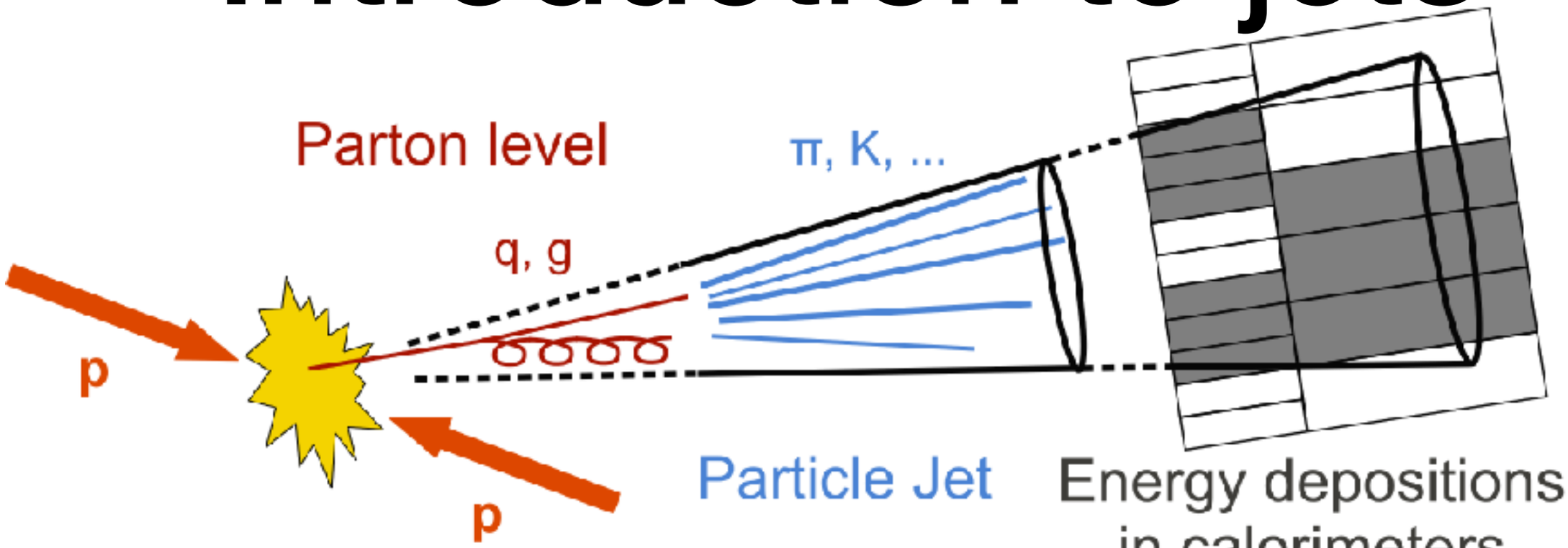

Jets are collimated sprays of hadrons arising from parton level interactions in colliding protons.

Jets are the dominant features arising in pp collisions at the LHC. Jets play a key role in many Standard Model physics analyses and searches of new phenomena. Jets are used to study the proton structure, strong coupling constants, and the non-perturbative effects of hadronisation and underlying events.

Jets are built:

- at the parton-level using partons knocked-out from protons
- at the particle-level using charged particles resulting in the parton evolution (hadronisation)
- at the reconstruction-level using calorimeter inputs (energy deposits in active cells) or tracks

Jets reconstruction in ATLAS

Jets are reconstructed in ATLAS using the Anti-k_t jet algorithm:

- Recombines all the entities (particles or calorimeter inputs), within a fixed cone of size ΔR=0.4, starting from the most energetic input.
- The algorithm is infrared and collinear safe.

The inputs for jets reconstruction in ATLAS are the topologically connected calorimeter cells, that contain a significant signal above noise (topoclusters).

The example of jet shapes in η-ϕ plane

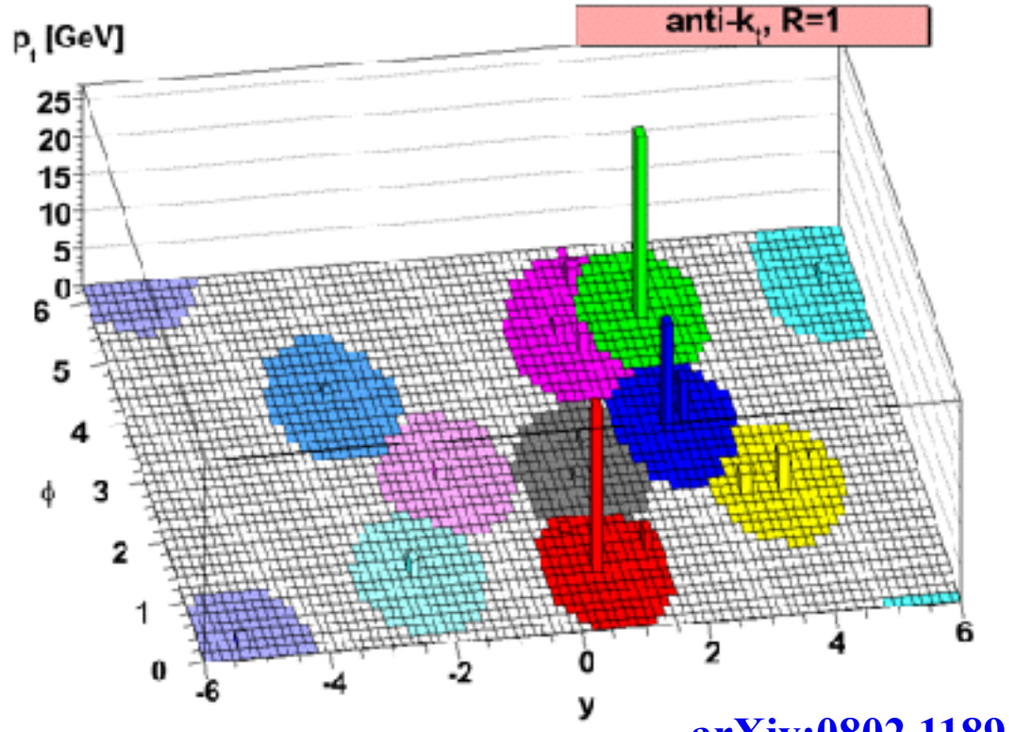

arXiv:0802.1189

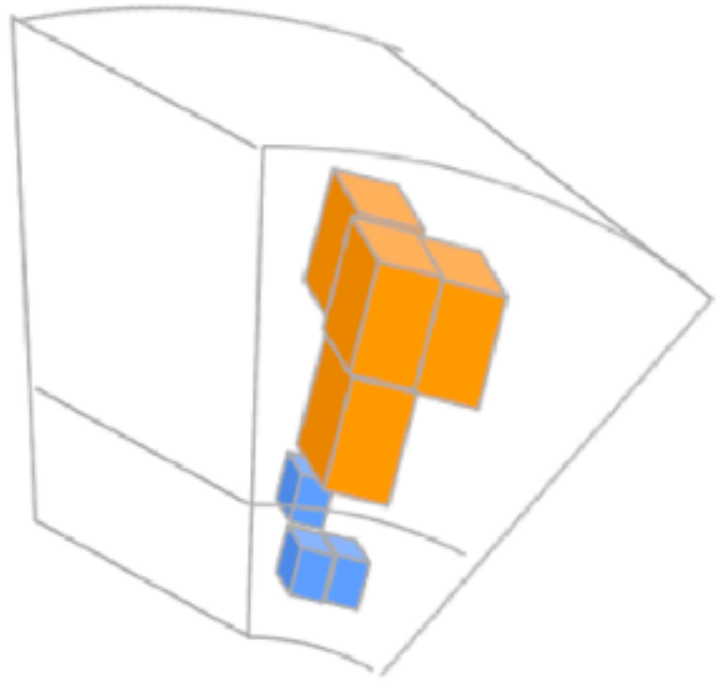

The energy scale of calorimeter cells is initially established for electromagnetic particles.

The local cell weighting (LCW) calibration is applied to clusters classified as hadronic to correct for different response to EM and hadronic particles, energy losses in inactive material and out-of-cluster energy deposits.

Jet energy scale (JES) calibration

- The jet energy scale (JES) calibration restores the energy scale of reconstructed jets to that of simulated truth jets.
- JES calibration consists of several consecutive stages derived from a combination of MC-based methods and in situ techniques.

EM-scale jets → **Origin correction** → **Jet area-based pile-up correction** → **Residual pile-up correction**

Jet finding applied to topological clusters at the EM scale.

Changes the jet direction to point to the hard-scatter vertex. Does not affect E.

Applied as a function of event pile-up p_T density and jet area.

Removes residual pile-up dependence, as a function of μ and N_{PV}.

Same for LCW jets

→ **Absolute MC-based calibration** → **Global sequential calibration** → **Residual *in situ* calibration**

Corrects jet 4-momentum to the particle-level energy scale. Both the energy and direction are calibrated.

Reduces flavor dependence and energy leakage effects using calorimeter, track, and muon-segment variables.

*A residual calibration is derived using in situ measurements and is applied **only to data**.*

The total JES uncertainty is below 1% for jets with $|\eta|<0.8$ in the $150\ \text{GeV} < p_T^{jet} < 1500\ \text{GeV}$ region.

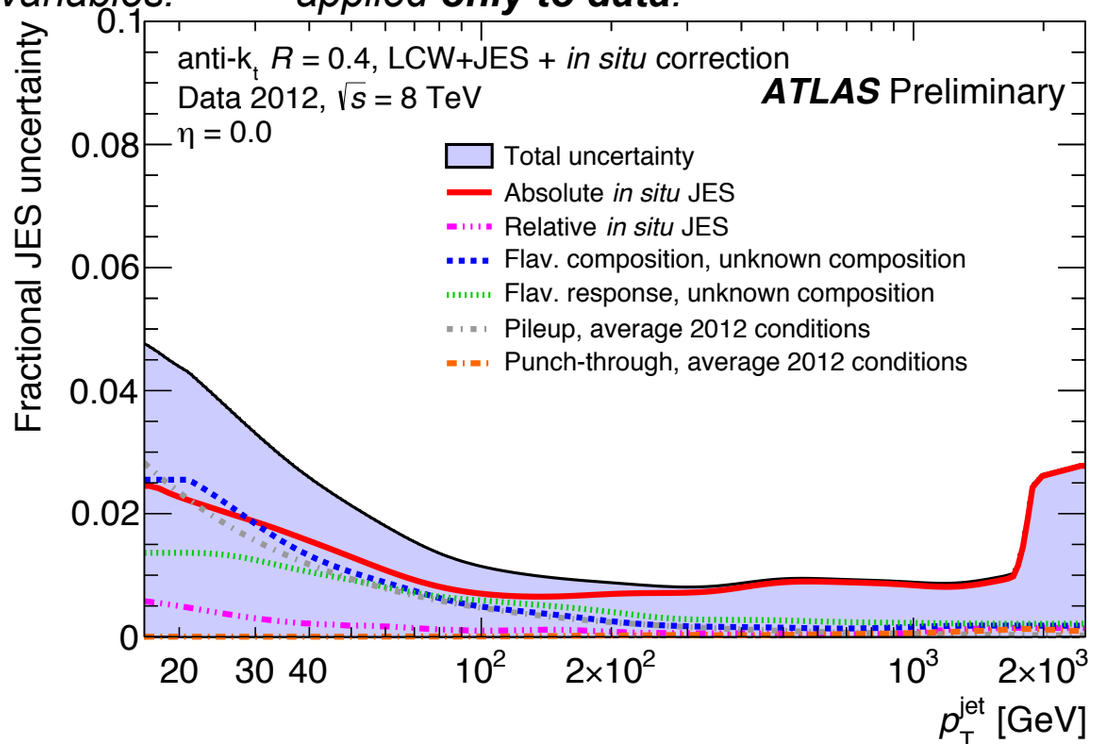

Z+jets NLO predictions

The NLO parton-level predictions are obtained using MCFM 6.8 interfaced to APPLgrid for fast convolution between different PDFs.

The CT14 PDF is used for NLO predictions. The strong coupling is 0.118. The renormalisation and factorisation scales are set equal to

$$\mu_r = \mu_f = \frac{\sqrt{m_{ee}^2 + p_{T,Z}^2} + \sum p_{T,\,partons}}{2}$$

The phase space definition:

- p_T^e>20 GeV, $|\eta^e|$<2.47,
- 66 GeV < M_{ee} < 116 GeV
- anti-k_t R=0.4 jets, p_T^{jet}>25 GeV, $|y_{jet}| < 3.4$

The uncertainty:

- Scales are varied by a factor of 2
- PDF uncertainty are assessed using supplementary error PDF sets
- The strong coupling of 0.116 and 0.120 are used

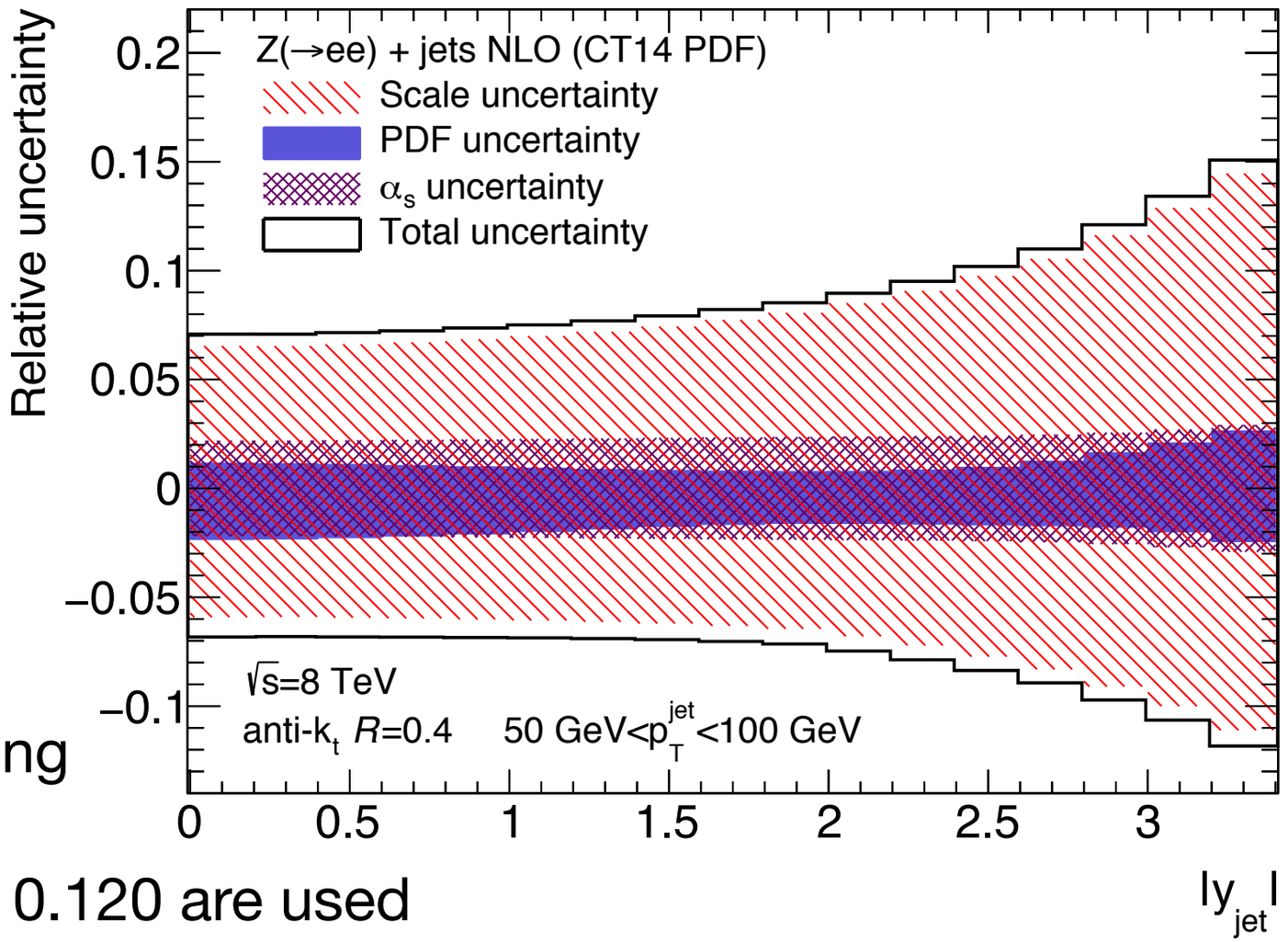

The result:

- Total uncertainty is 6-20%, dominated by the scales. The pdf and alphas uncertainties are 2-5%.

Z+jets NNLO predictions

The state-of-the-art NNLO predictions are available from 2016. The calculations are done by different groups: A. Gehrmann-De Ridder et al. and R. Boughezal et al.

The NNLO predictions are provided to us by A. Gehrmann-De Ridder et al.

The result:

- The NLO/NNLO k-factor increases as the function of the jet pt and jet eta from 3% to 15%.
- Scale uncertainty is significantly reduced. Total uncertainty is 2-5%.

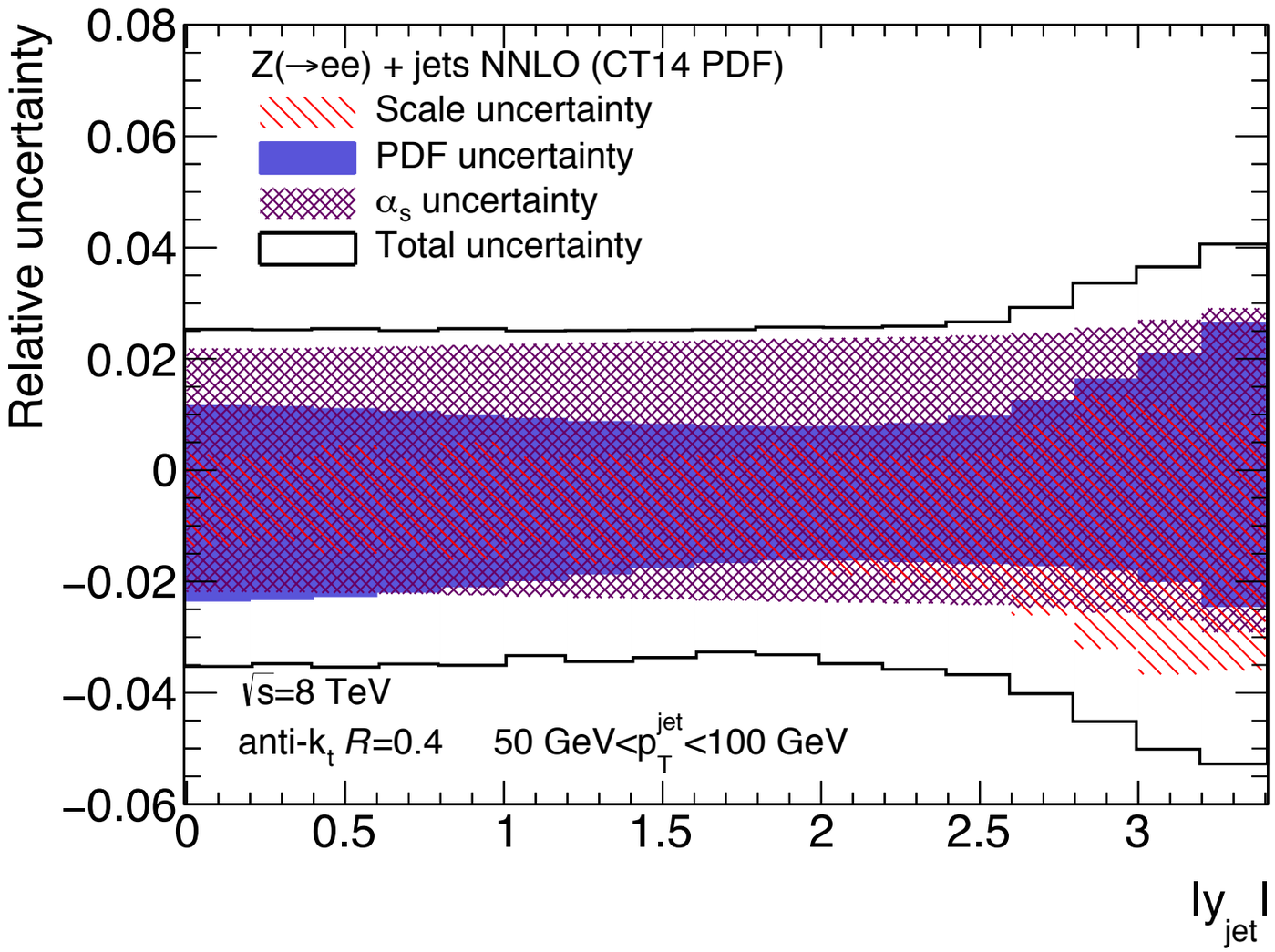

PDF variations

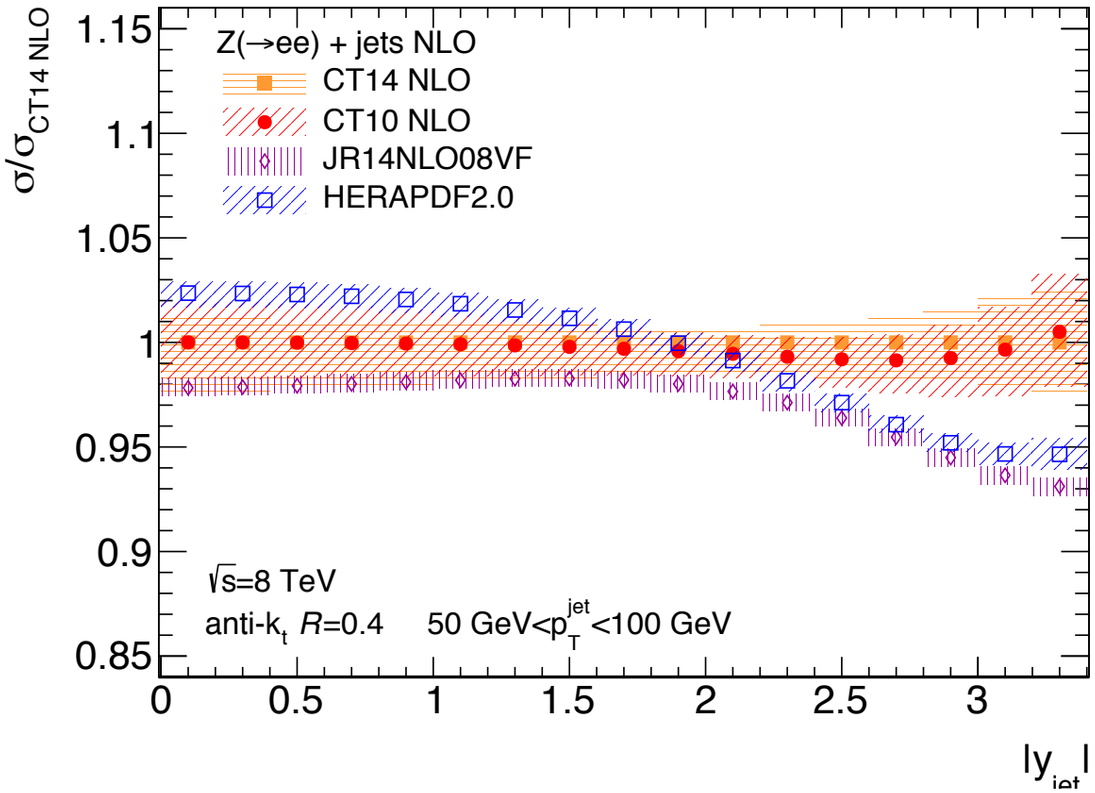

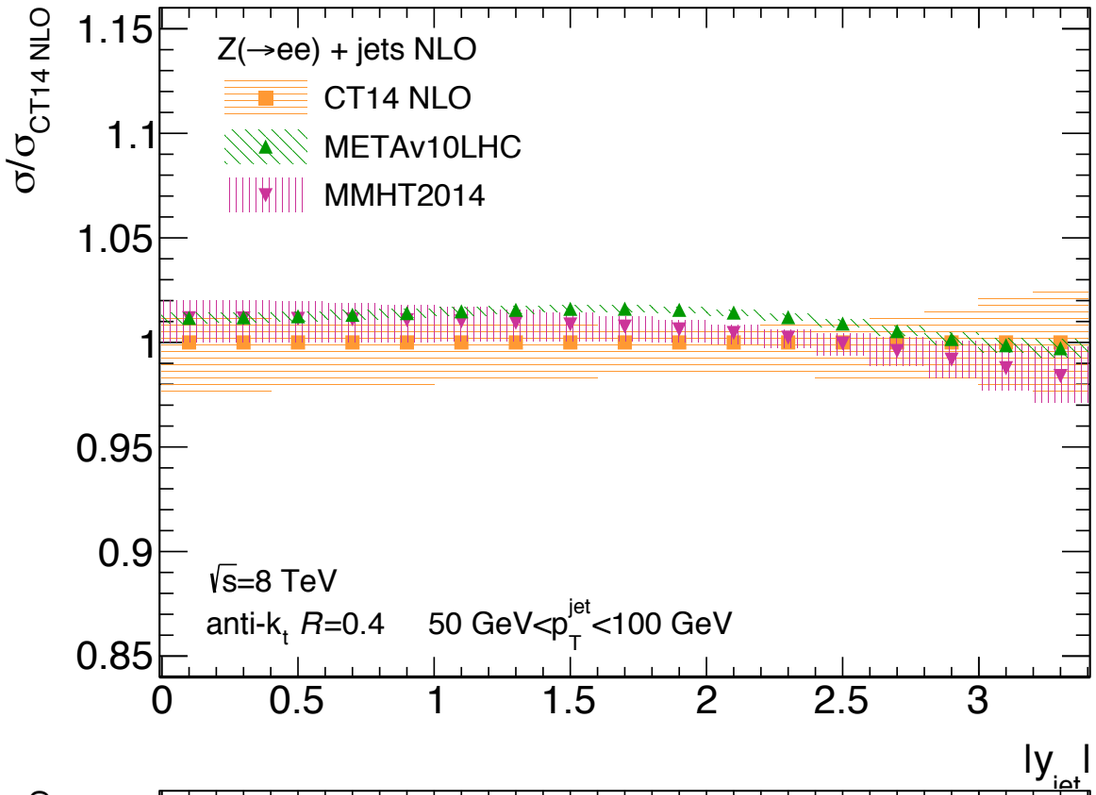

- NLO predictions are obtained with different PDFs. Only PDF uncertainties are shown.
- The study shows up to 10% difference in Z+jets cross-sections calculated with different PDFs. This shows the PDF sensitivity of the measurement.

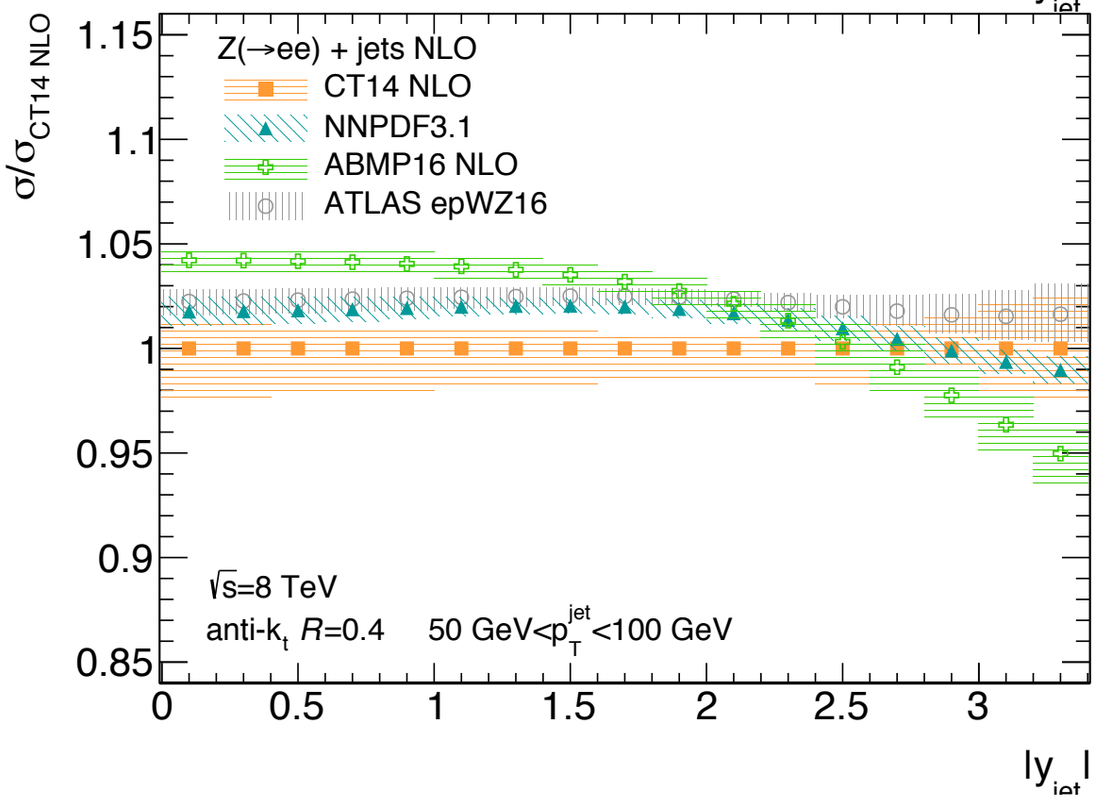

Non-perturbative correction

The theory predictions, obtained at parton level, are corrected by hadronisation and underlying events.

The non-perturbative correction:

$$k_{\mathrm{NP}} = \left.\frac{\frac{d^2\sigma}{d\,|y^{\mathrm{jet}}|\,dp_{\mathrm{T}}^{\mathrm{jet}}}}{\frac{d^2\sigma}{d\,|y^{\mathrm{jet}}|\,dp_{\mathrm{T}}^{\mathrm{jet}}}}\right|_{\mathrm{NP\ off}}^{\mathrm{NP\ on}}$$

- The correction (obtained with Sherpa) is up to 10% in the first p_T^{jet} bin for forward jets, vanishing at higher p_T^{jet} bins.
- Uncertainty is 5-10%, obtained as the envelope of k_{NP} obtained with different MC generators and tunes

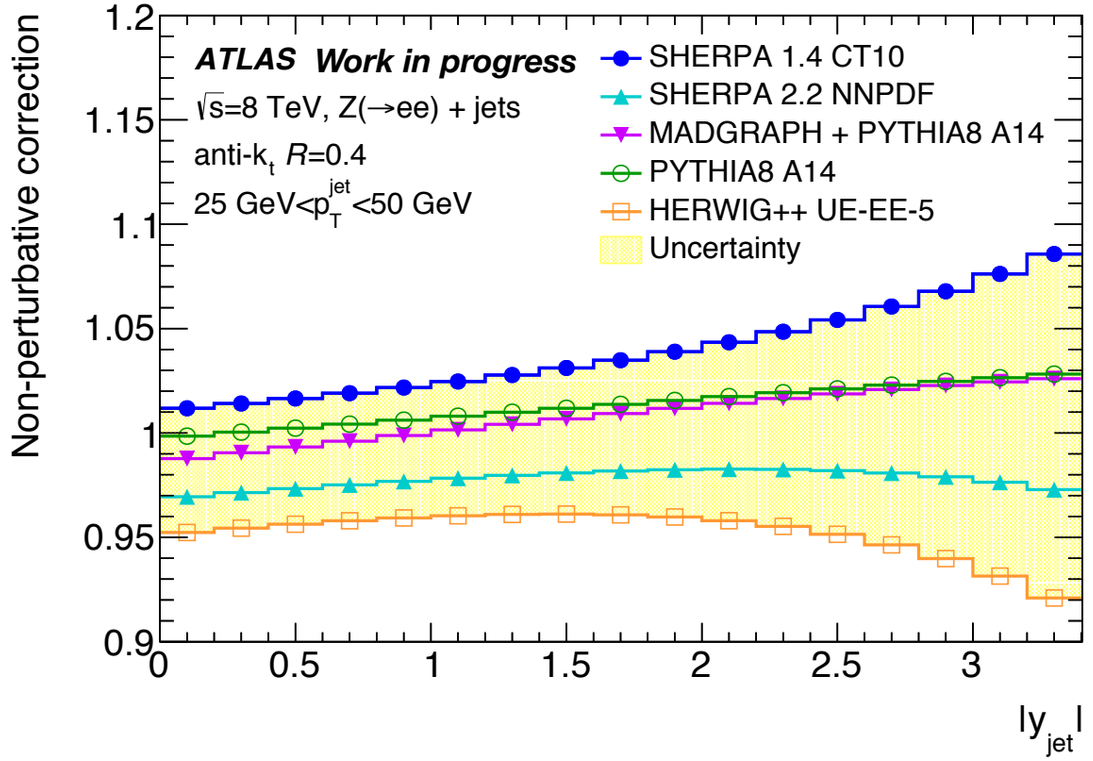

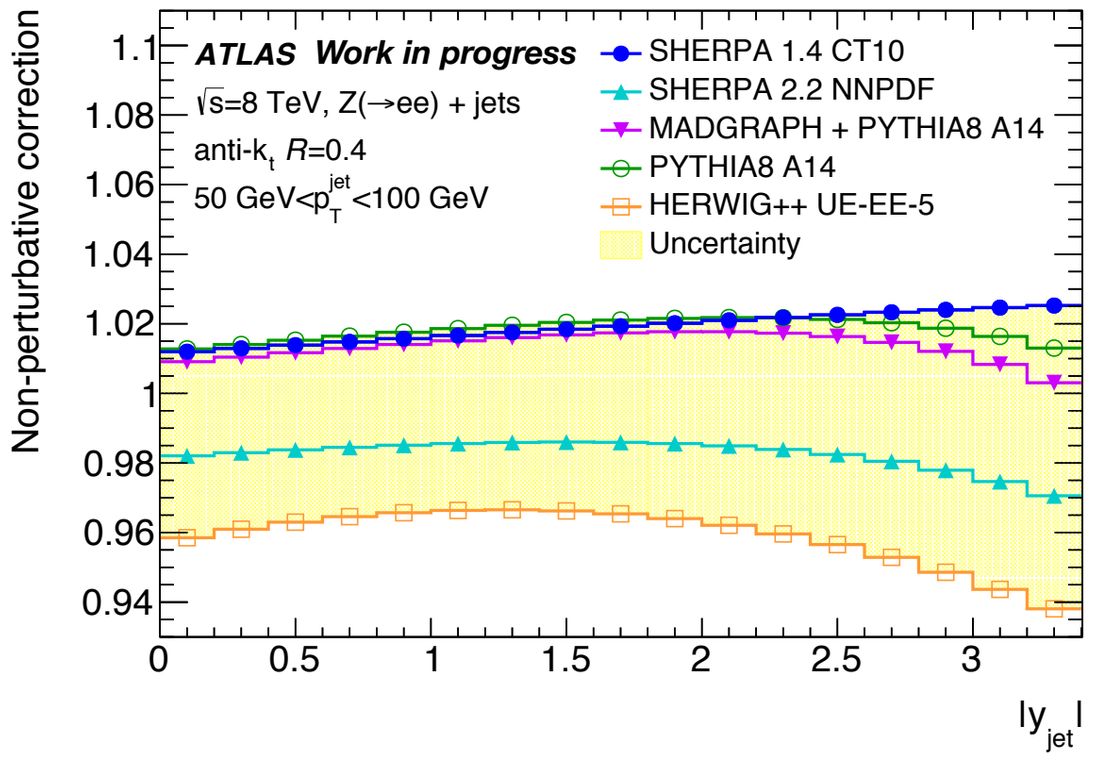

$Z \rightarrow ee$ + jets selection

Event selection:

- Events are triggered by dielectron triggers
- Number of tracks in primary vertex ≥ 3
- Events recorded with any detector subsystem being non-operational are excluded

Electron selection:

- Two opposite side reconstructed electrons
- Medium electron identification
- p_T^e>20 GeV, $|\eta^e|$<2.47 (excl. 1.37<$|\eta^e|$<1.52)
- 66 GeV < M_{ee} < 116 GeV

Data sample:

- **20.1 fb^{-1} 8 TeV pp collision ATLAS data.**

ME+PS MC predictions with full detector simulations are:

- **Sherpa 1.4**
- **Alpgen + Pythia 6**

Jets selection:

- anti-k_t R=0.4 jets are built using LCW topoclusters
- $|y_{jet}| < 3.4$, p_T^{jet}>25 GeV (p_T^{jet} bin edges are 25,50,100,200,300,400,1050 GeV)
- ΔR(jet,electron) ≤ 0.4
- Jets originating from pile-up vertices are excluded
- Jets from non-collision backgrounds and jets falling in non-operational detector regions (bad jet quality) are rejected.

Background analysis

The backgrounds are:

- $Z \rightarrow \tau\tau$ ($\tau \rightarrow e\nu$)
- Dibosons production (WW, ZZ, WZ bosons decay in electron channel)
- Single top-quark and ttbar ($\tau \rightarrow Wb$)
- W+jets (one electron from W decay, and another is jet misidentified as electron)
- Multijet (two jets are misidentified as electrons)

Simulated backgrounds

Combined background is estimated with the data-driven method

Data-driven background is estimated using a shape template obtained from data using background enhanced selection:

- Data sample selected with single electron triggers
- Inverted electron identification criteria
- Same charge electrons

The template is obtained subtracting the simulated Z+jets signal and backgrounds events from data.

We use M_{ee} distribution as a discriminating variable. The M_{ee} template is then fit to the Z+jets data in enlarged M_{ee} window to asses larger background at the tails fo the M_{ee} distribution.

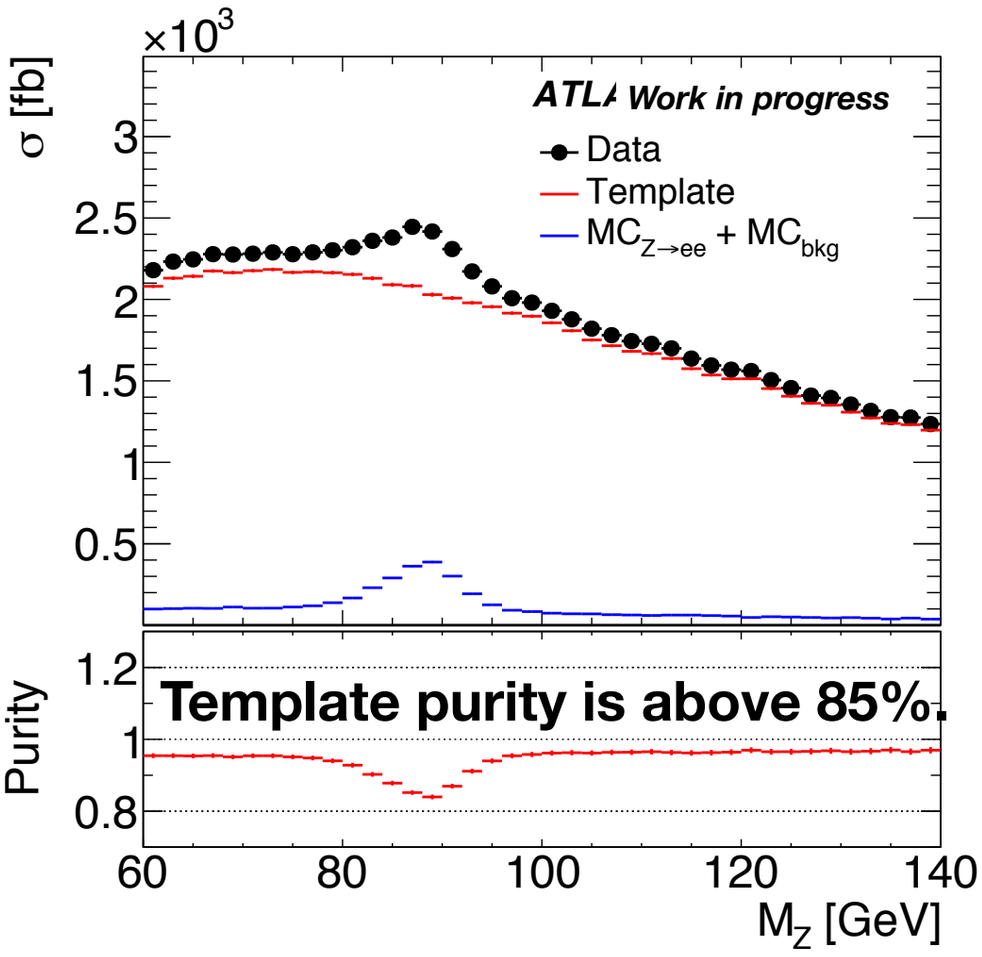

Background results

- The ttbar background of 0.5-8% is the dominant in most of bins increasing for higher jet pt and rapidity
- The W+jets and multijet background is 1-3%. Dominates in the low jet pt region.
- The dibosons background is about 0.5% in all bins of the measurement.
- The Z→ττ and single-top quark backgrounds are below 0.1%.

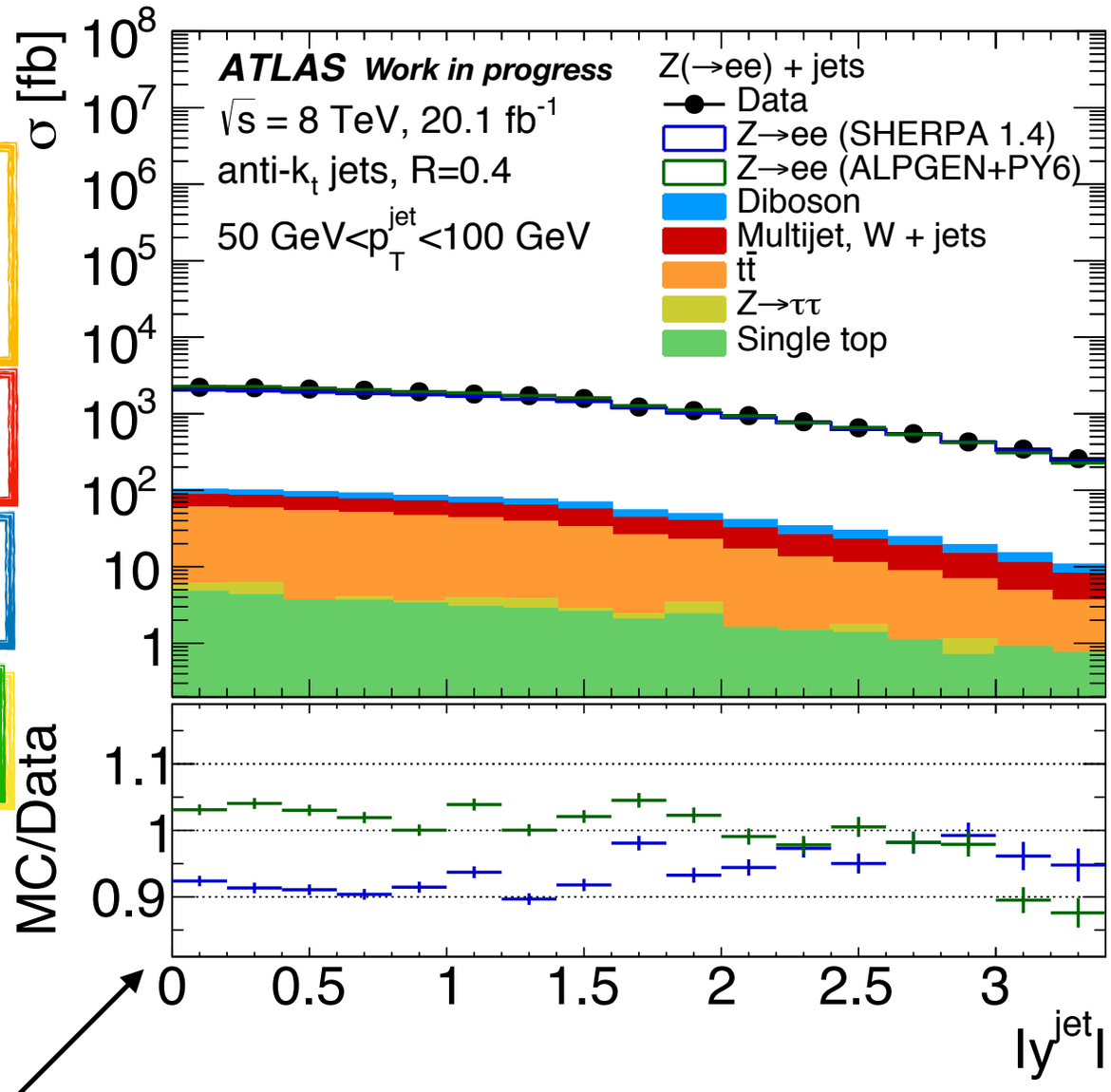

The data/MC differences are covered by the uncertainties that are discussed later in the talk.

Unfolding and cross section measurement

The experimental measurements are affected by the detector resolution and reconstruction inefficiencies. We use iterative Bayesian unfolding to correct for these detector effects.

- The backgrounds are subtracted from data prior the unfolding
- The unfolded number of jets (at the particle-level) in data is obtained as

$$N_i^{\mathrm{P}} = \frac{1}{\mathscr{E}_i^{\mathrm{P}}} \sum_j U_{ij} \mathscr{E}_j^{\mathrm{R}} N_j^{\mathrm{R}}$$

where N^R is the number of reconstructed jets, while U, $\mathscr{E}^R$ and $\mathscr{E}^P$ are the inputs for the unfolding.

- $\mathscr{E}^R$ and $\mathscr{E}^P$ are the reconstructed-level and particle-level matching efficiencies
- the U is the transfer matrix that accounts for the bin-to-bin migrations

The U, $\mathscr{E}^R$ and $\mathscr{E}^P$ are improved using two unfolding iterations to reduce the impact of the particle level jet spectra.

The double differential Z+jets cross sections are then calculated as

$$\frac{d^2\sigma}{dp_{\mathrm{T}}^{\mathrm{jet}} d\,|y^{\mathrm{jet}}|} = \frac{1}{\mathscr{L}} \frac{N_i^{\mathrm{P}}}{\Delta p_{\mathrm{T}}^{\mathrm{jet}} \Delta\,|y^{\mathrm{jet}}|}$$

where $\mathscr{L}$ is the luminosity, and Δp_T^{jet} and $\Delta|y_{jet}|$ are the bin widths.

Experimental uncertainties

- **JER uncertainty** 5-15% is the dominant in the first p_T^{jet} bin ($25 < p_T^{jet} < 50$ GeV). In larger p_T^{jet} bins it reduces to 0.5-3%.
- **JES uncertainty** is the second dominant in the first p_T^{jet} bin, 5-15%. But it is dominant in larger p_T^{jet} bins, 2-6%.
- **Other** uncertainties are generally below 2%.
  - **unfolding uncertainty** is the dominant of them in first p_T^{jet} bin (up to 7%), but it is below 1% in larger p_T^{jet} bins.
  - **data-driven background uncertainty** is generally about 1-2%.
  - **electron** related uncertainties are generally below 1%.
  - **jet quality uncertainty** of 1% is assigned to in all p_T^{jet} bins.
- **Statistical uncertainty** increases from 0.5-1.5% in first p_T^{jet} bin to 10-15% in last p_T^{jet} bin.
- The luminosity uncertainty of 1.9% is not shown.

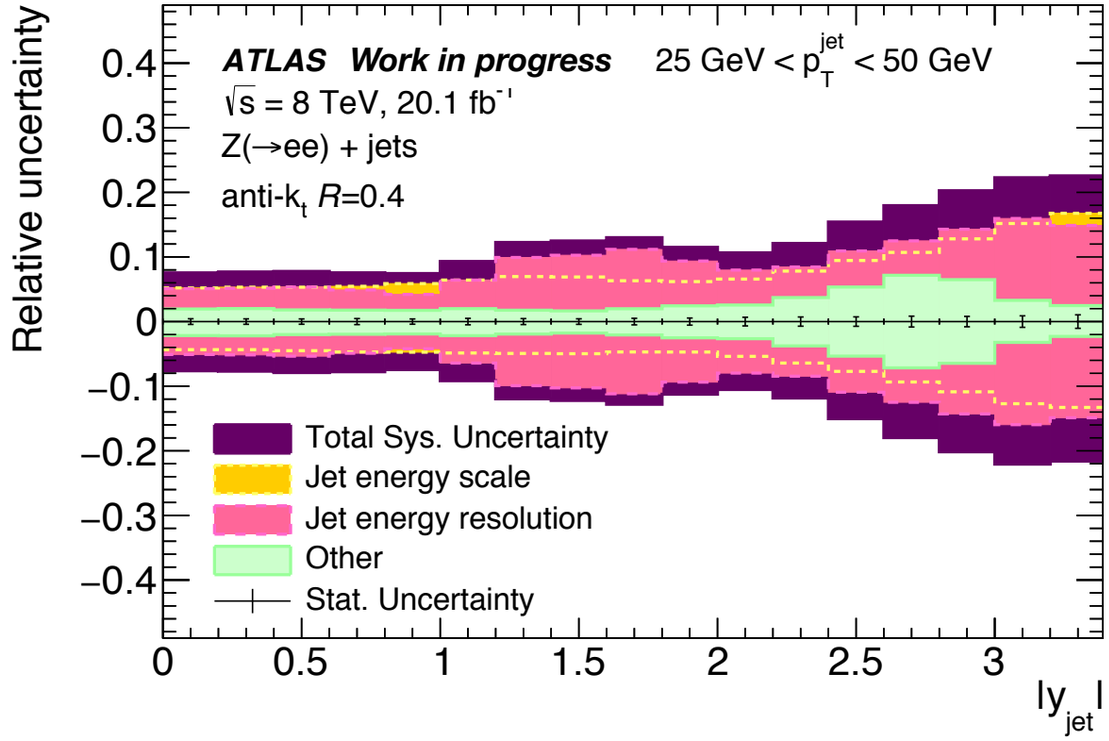

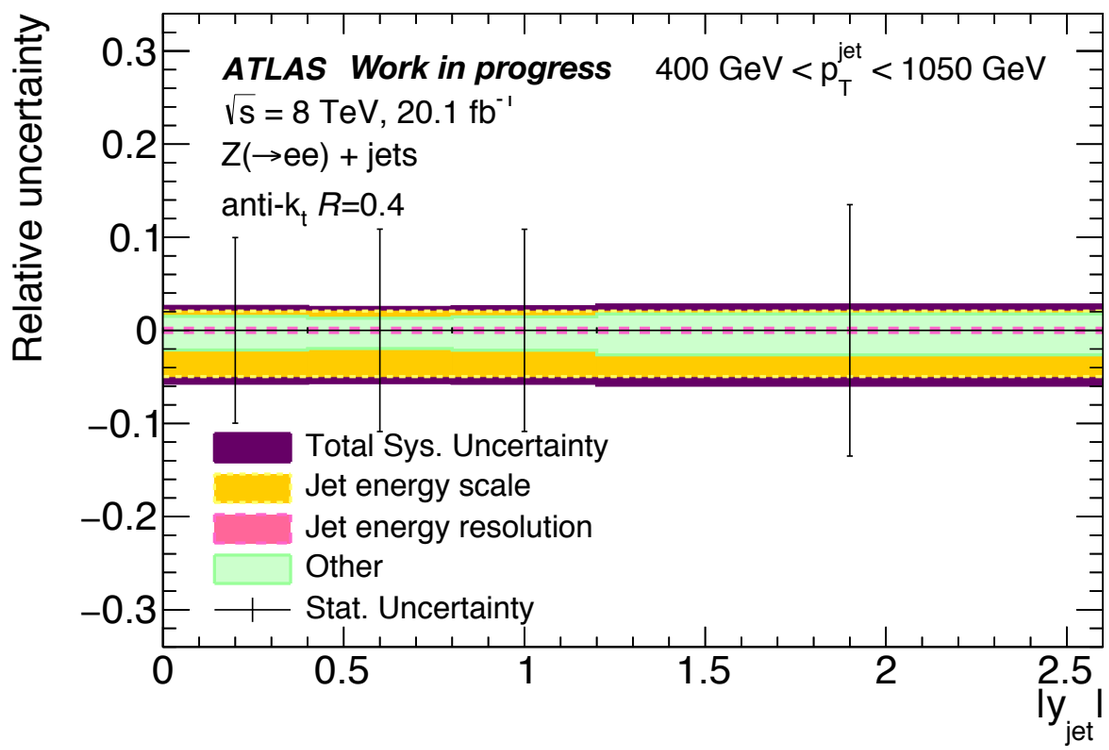

Results

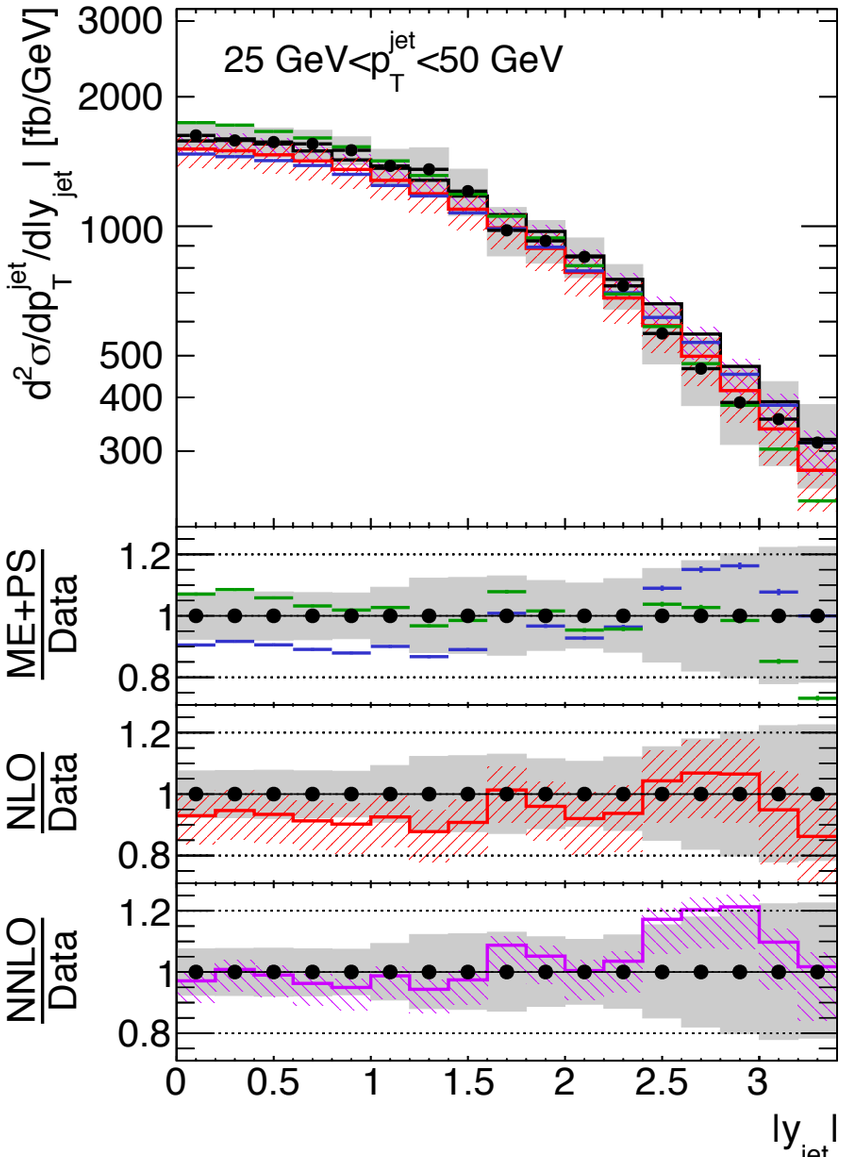

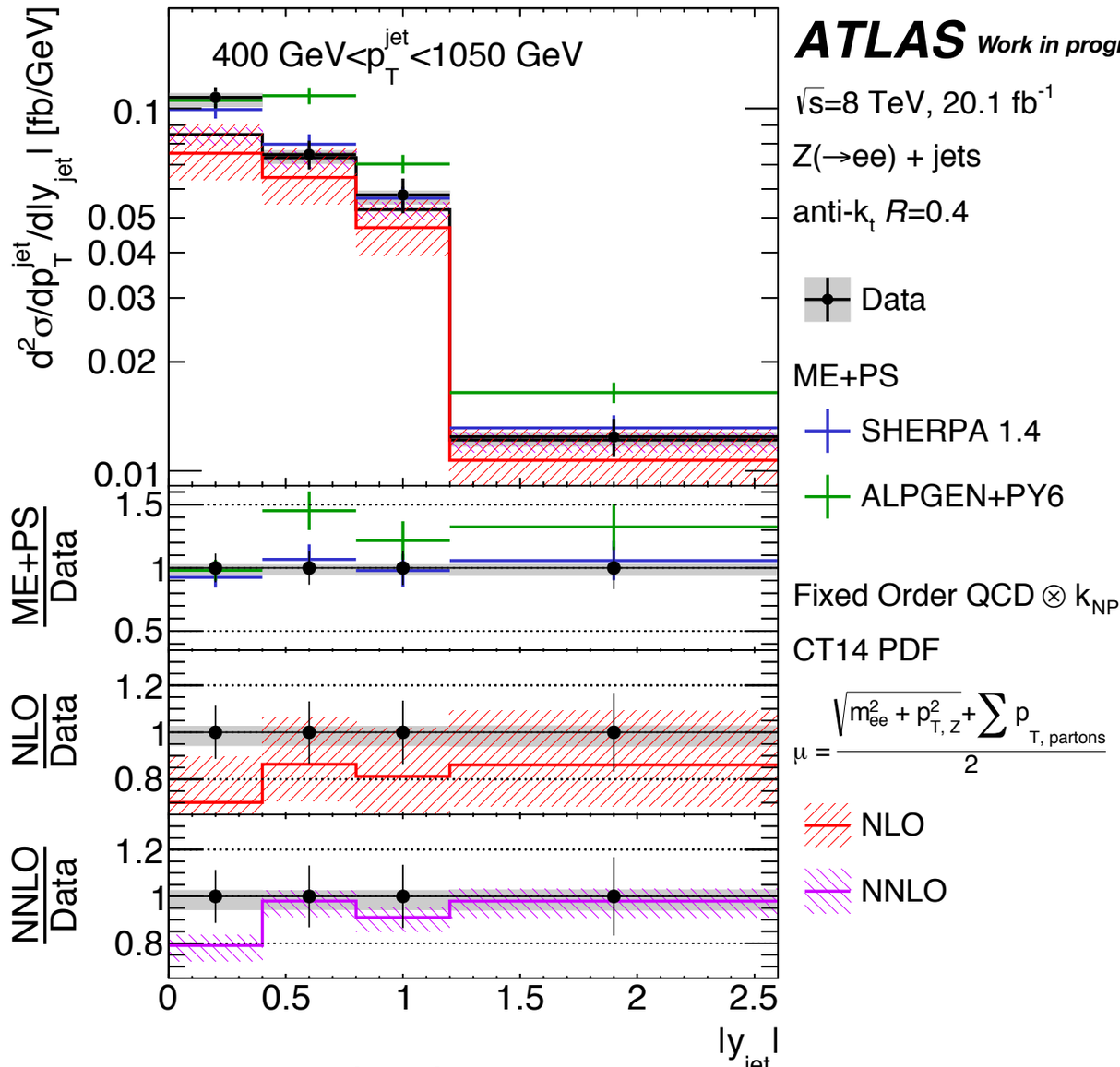

The cross-sections cover 5 orders of magnitude and falls vs $|y_{jet}|$ and p_T^{jet}

- **Sherpa** predictions underestimates data by 10% in low p_T^{jet} bins. In high p_T^{jet} bins it describes data well.
- **Alpgen+Pythia** describes data well in low p_T^{jet} bins, but overestimates data by 20% in high p_T^{jet} bins.
- **NLO** underestimates data by few percents.
- **NNLO** is in best agreement with data in all bins of the measurement.

The observed data/MC differences are covered by the experimental uncertainties.

Summary

- The Z+jets double differential cross sections are measured using the 20 fb^{-1} ATLAS pp collisions data.
- The results are in good agreement with the ME+PS and fixed order theory predictions. The best agreement is observed with the NNLO predictions.
- The uncertainties of the measured cross sections are about twice lower than that in NLO predictions and are approximately equal to the uncertainties in NNLO calculations.
- The measurement provides a precision inputs to constrain the parton distribution function, especially for gluons.

Backup

Z -> mu mu + 3 jets event display

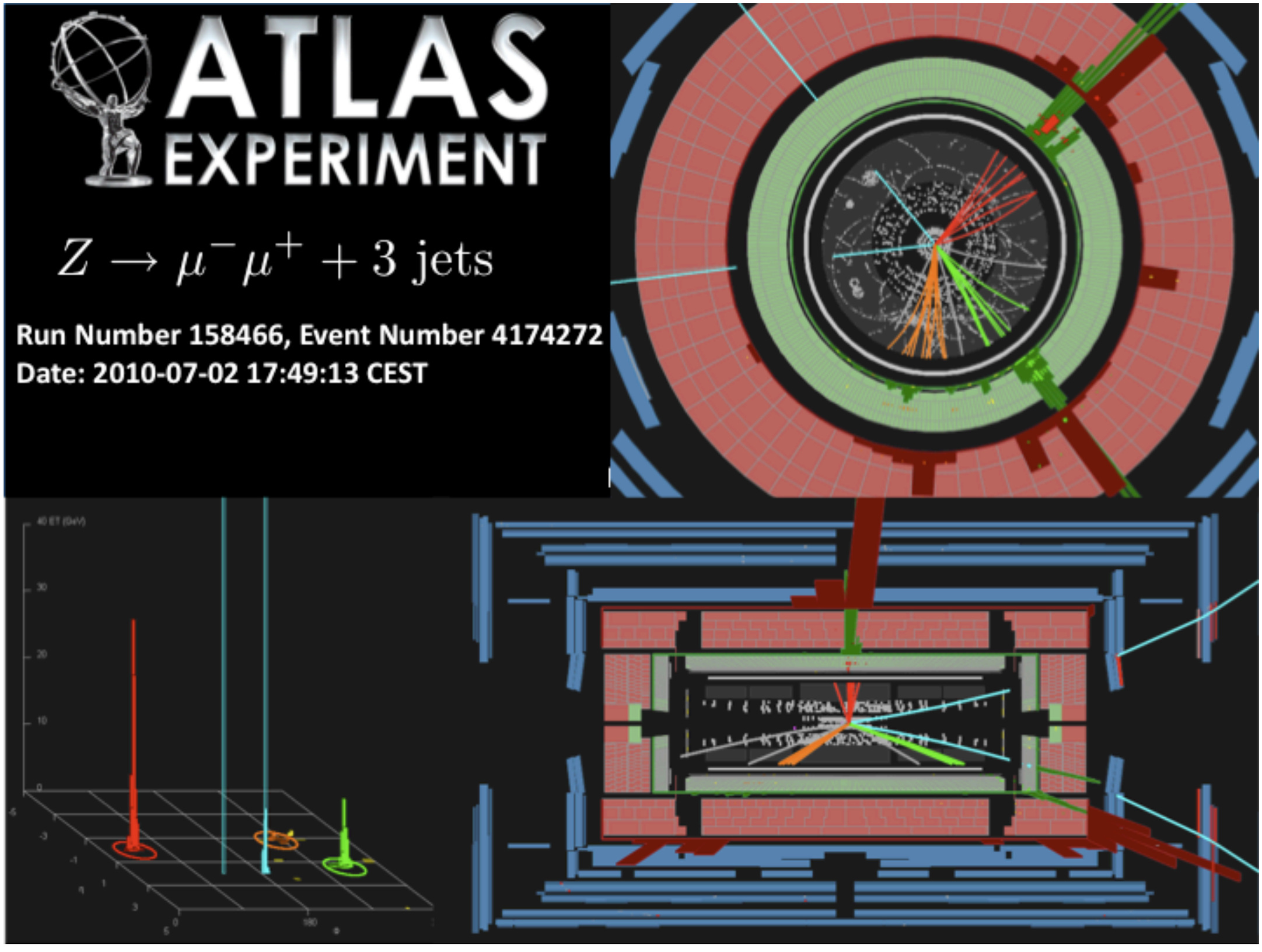

Z -> ee event display

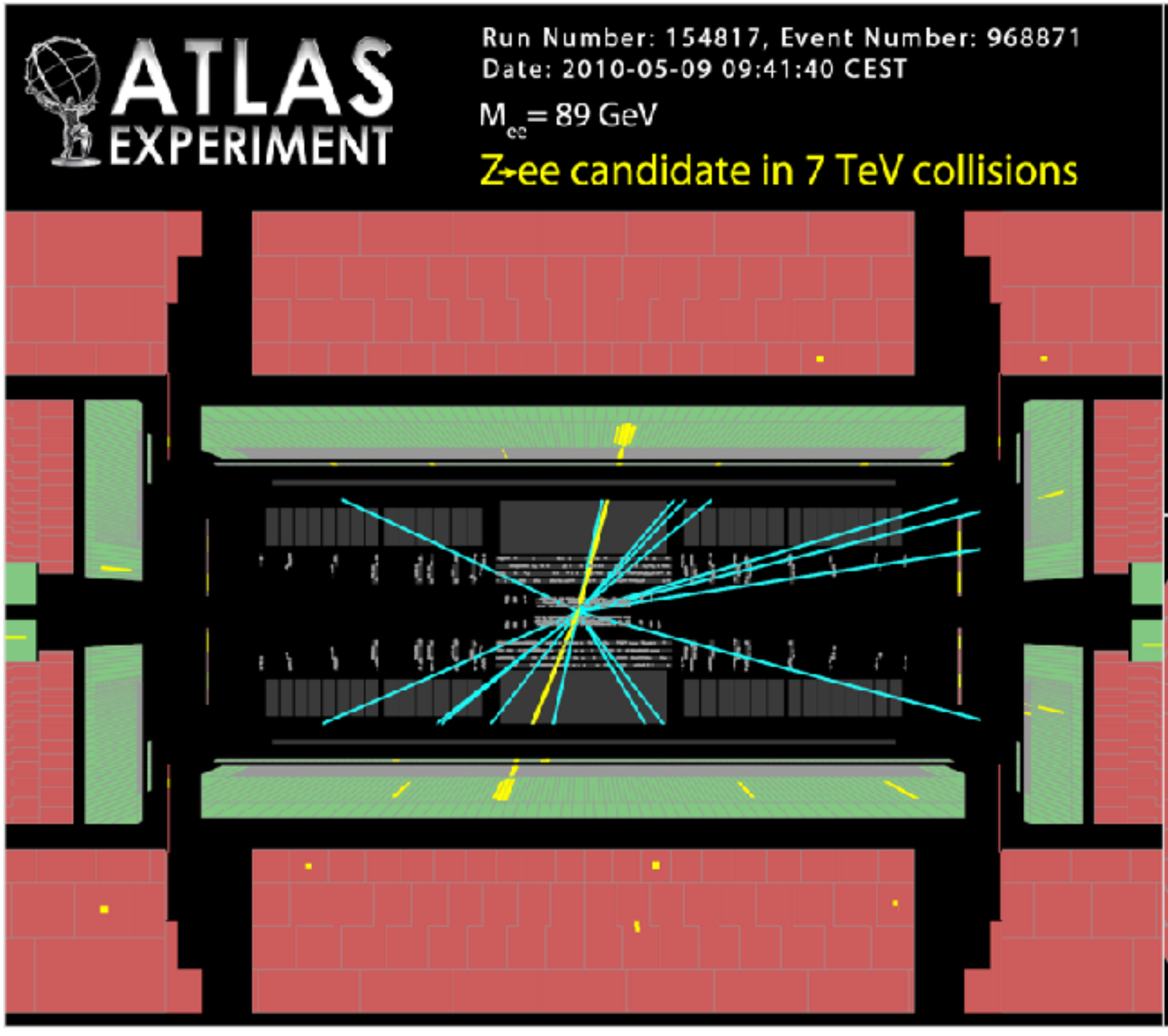

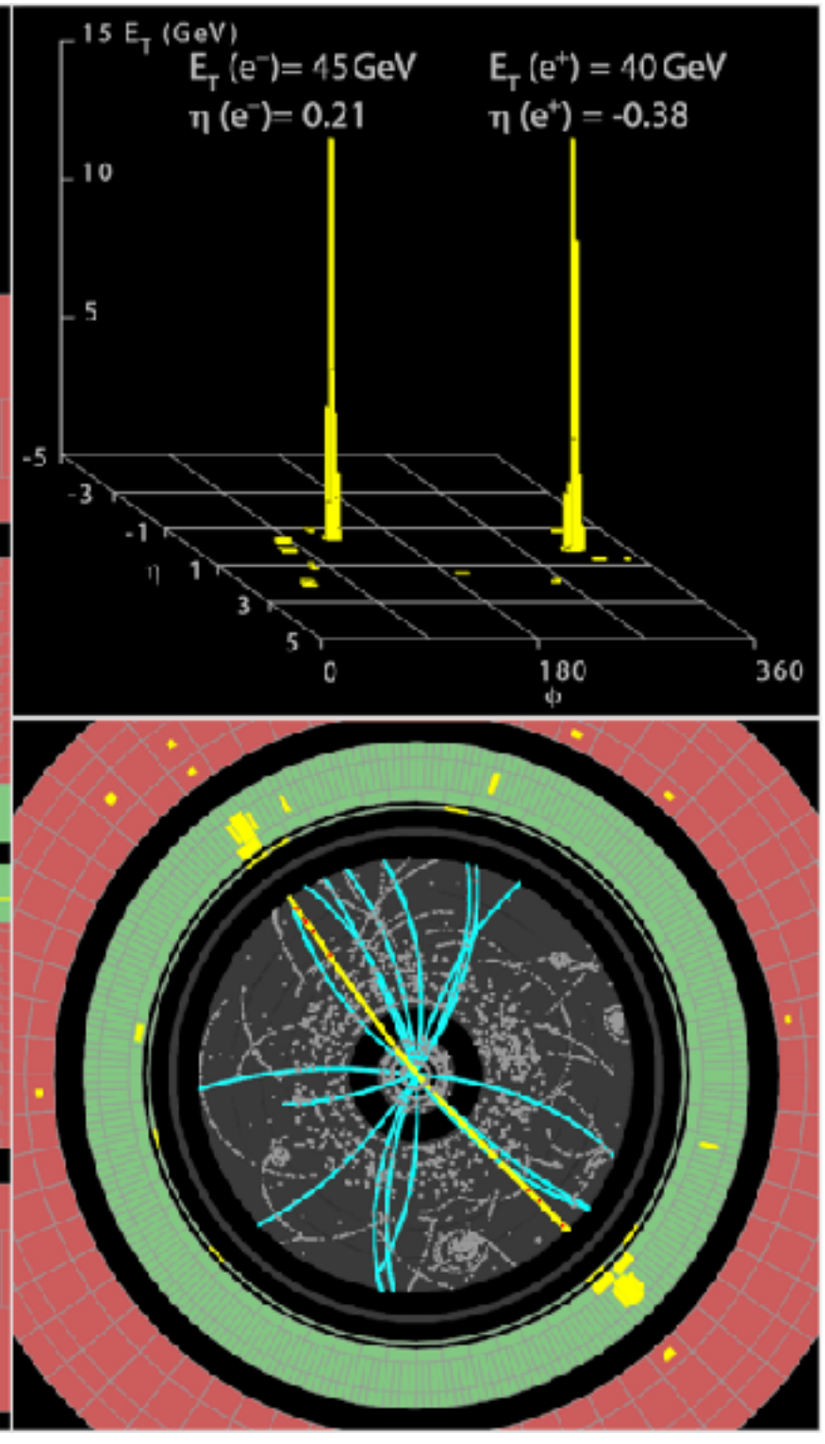

6 jets event display

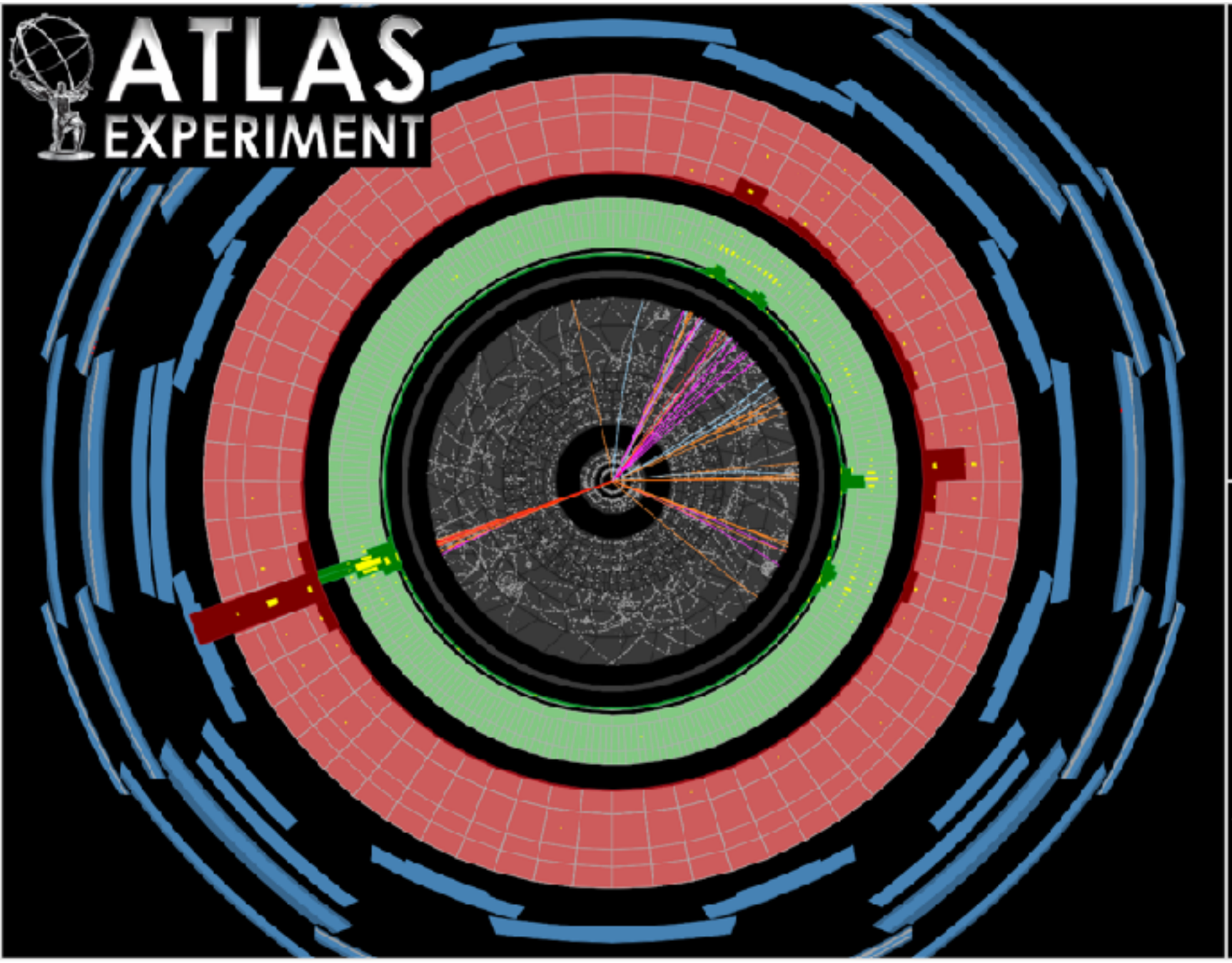

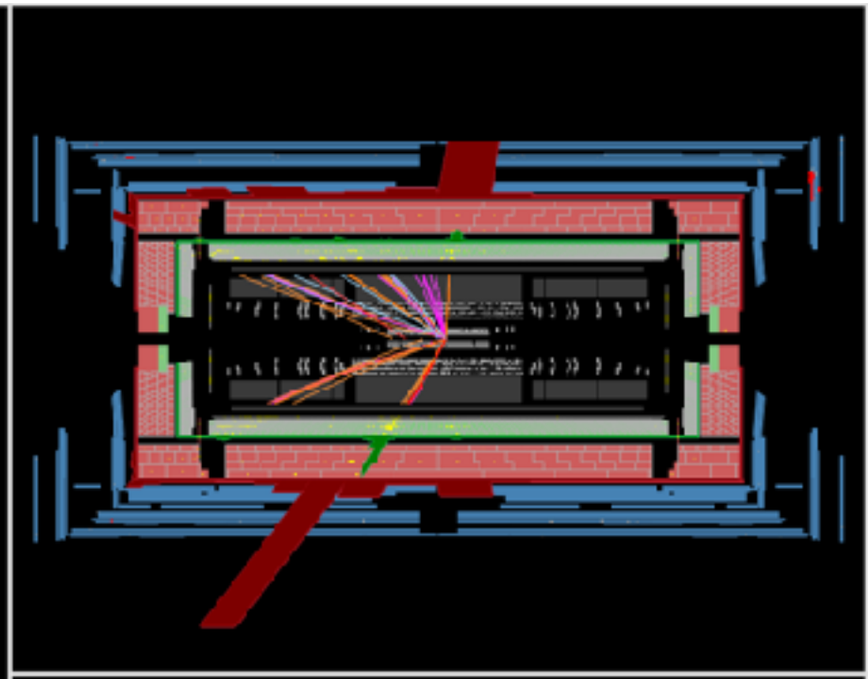

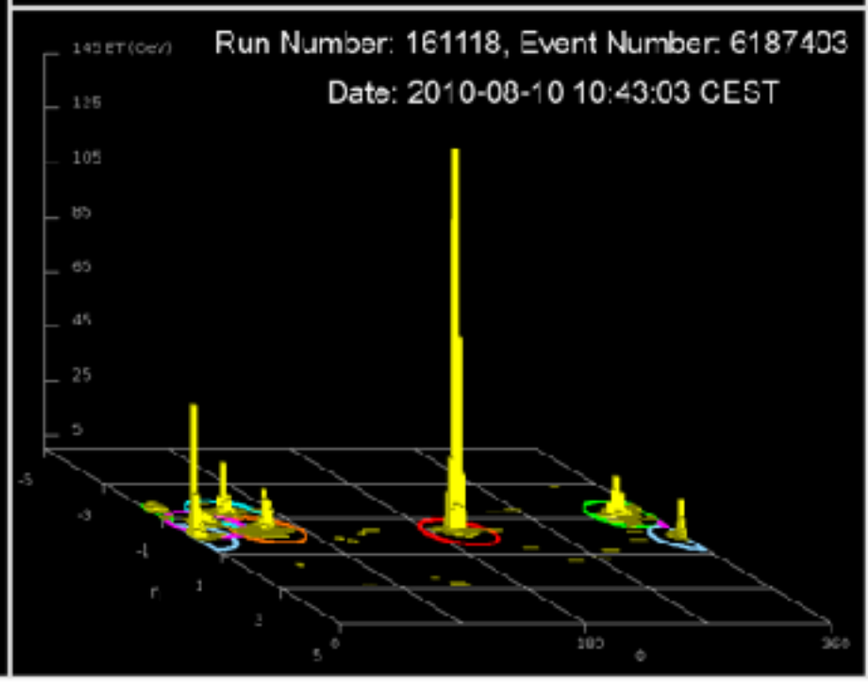

Electromagnetic calorimeter

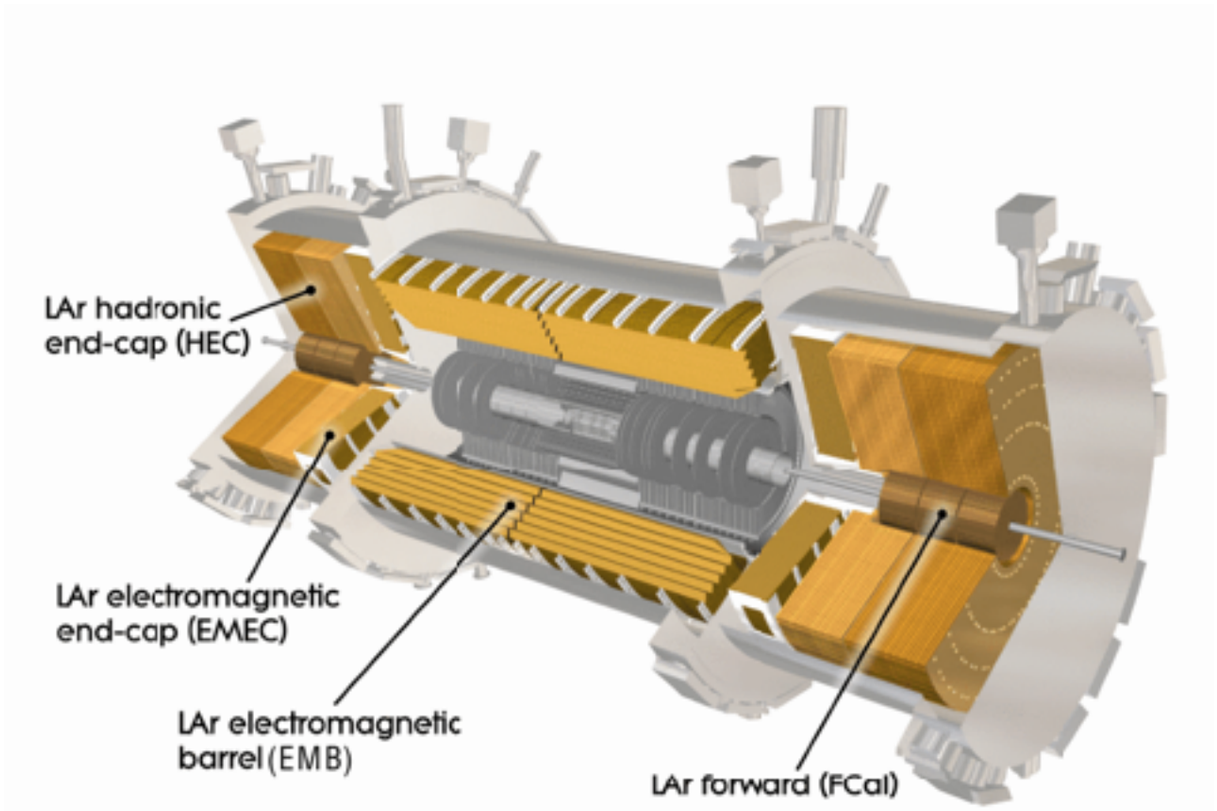

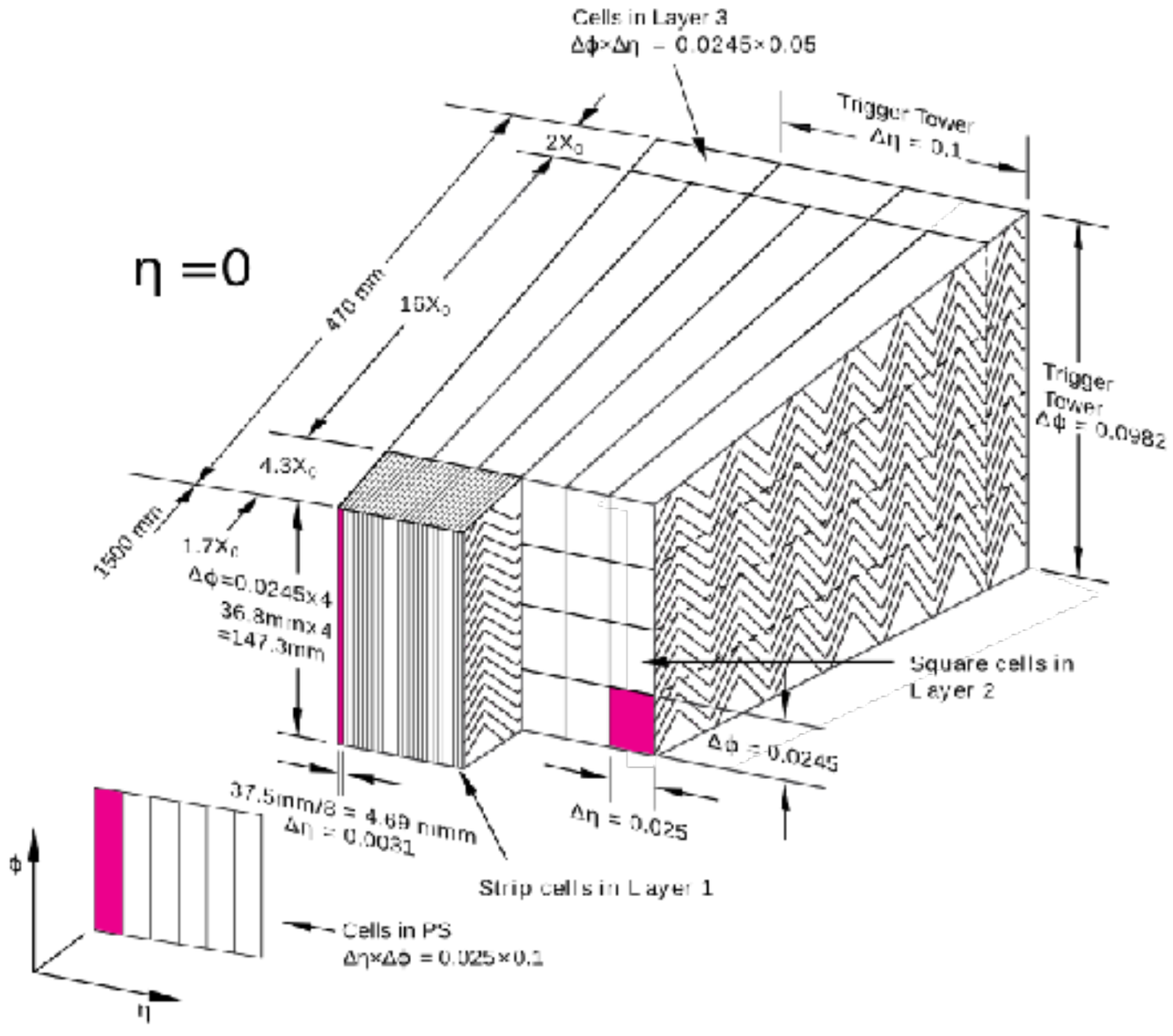

Hadronic calorimeter